



Published in final edited form as:

Stem Cells. 2009 September ; 27(9): 2301–2311. doi:10.1002/stem.165.

## Fibroblastic Colony-Forming Unit Bone Marrow Cells Delay Progression to Gastric Dysplasia in a *Helicobacter* Model of Gastric Tumorigenesis

Sophie S.W. Wang<sup>a,b,c</sup>, Samuel Asfaha<sup>a</sup>, Tomoyuki Okumura<sup>a</sup>, Kelly S. Betz<sup>a</sup>, Sureshkumar Muthupalani<sup>d</sup>, Arlin B. Rogers<sup>d</sup>, Shuiping Tu<sup>a</sup>, Shigeo Takaishi<sup>a</sup>, Guangchun Jin<sup>a</sup>, Xiangdong Yang<sup>a</sup>, Deng-Chyang Wu<sup>b,c</sup>, James G. Fox<sup>d</sup>, and Timothy C. Wang<sup>a</sup>

<sup>a</sup>Division of Digestive and Liver Diseases, Columbia University Medical Center; New York, New York, USA

<sup>b</sup>Graduate Institute of Medicine, Kaohsiung Medical University, Kaoshing, Taiwan

<sup>c</sup>Division of Gastroenterology, Department of Internal Medicine, Kaohsiung Medical University Hospital, Kaoshing, Taiwan

<sup>d</sup>Division of Comparative Medicine, Massachusetts Institute of Technology, Cambridge, Massachusetts, USA

### Abstract

Bone marrow mesenchymal stem cells (MSCs) have been shown to have immune modulatory effects. Despite efforts to identify these cells *in vivo*, to date, MSCs have been defined mainly by their *in vitro* cell characteristics. Here, we show that Lin<sup>-</sup>CD44<sup>hi</sup>Sca1<sup>-</sup>cKit<sup>+</sup>CD34<sup>-</sup> cells make up ~0.5%–1% of murine whole bone marrow cells and yield nearly an equal amount of fibroblastic colony-forming units (CFU-F) as whole bone marrow. After transplantation into lethally irradiated recipients, Lin<sup>-</sup>CD44<sup>hi</sup>Sca1<sup>-</sup>cKit<sup>+</sup>CD34<sup>-</sup> cells engrafted in the bone marrow long-term and demonstrated characteristics of MSCs, including capacity to differentiate into osteoblasts and adipocytes. To examine whether Lin<sup>-</sup>CD44<sup>hi</sup>Sca1<sup>-</sup>cKit<sup>+</sup>CD34<sup>-</sup> cells have immune modulatory effects, *in vitro* coculture with activated CD4<sup>+</sup> T-cells resulted in decreased Th17 cell differentiation by Lin<sup>-</sup>CD44<sup>hi</sup>Sca1<sup>-</sup>cKit<sup>+</sup>CD34<sup>-</sup> cells. Furthermore, serial infusions with Lin<sup>-</sup>CD44<sup>hi</sup>Sca1<sup>-</sup>cKit<sup>+</sup>CD34<sup>-</sup> cells reduced the progression to low-grade gastric dysplasia in mice infected with chronic *Helicobacter felis* ( $p = .038$ ). This correlated with reduced gastric interleukin (IL)-17F, IL-22, and ROR- $\gamma$ t gene expression in responding mice ( $p < .05$ ). These data suggest that bone marrow derived Lin<sup>-</sup>CD44<sup>hi</sup>Sca1<sup>-</sup>cKit<sup>+</sup>CD34<sup>-</sup> cells have characteristics of MSCs and reduce progression of early gastric tumorigenesis induced by chronic *H. felis* infection. The prevention of dysplastic changes may occur through inhibition of Th17-dependent pathways.

© AlphaMed Press

Correspondence: Timothy C. Wang, M.D., 1130 St. Nicholas Avenue, Room 925, New York, NY 10032, USA. Telephone: 212-851-4581, Fax: 212-851-4590; tcw21@columbia.edu.

Author contributions: S.W., D.W., T.C.W.: designed the study; S.W., S.A., T.O., Sp.T., S.T., G.J., X.Y., K.B.: performed all the experiments; S.M., A.B.R., J.G.F: performed histology scoring; S.W., S.A., D.W., T.C.W: wrote the manuscript.

**DISCLOSURE OF POTENTIAL CONFLICTS OF INTEREST** The authors indicate no potential conflicts of interest.

See [www.StemCells.com](http://www.StemCells.com) for supporting information available online.

## Keywords

Bone marrow; Nonhematopoietic; Fibroblastic colony-forming units; Mesenchymal stem cells; Cellular immunity; Th17; Inflammation-induced carcinogenesis; Immune modulation; *Helicobacter felis*; Gastric dysplasia; Gastric tumorigenesis

---

## Introduction

Bone marrow–derived mesenchymal stem cells (MSCs) have been shown to be effective in the treatment of various conditions in both animal models and humans [1,2]. MSCs are defined by several criteria, including plastic adherence when maintained in standard culture conditions; expression of nonhematopoietic cell surface markers; and capacity to differentiate to osteoblasts, adipocytes, and chondrocytes [3–7]. However, despite attempts to identify this cell population in vivo, it has proven challenging to isolate MSCs due to the lack of identification of distinguishing cell surface markers. Recent human studies have shown that CD146<sup>+</sup> pericytes within the bone marrow and other organs such as skeletal muscle, white adipose tissue, pancreas, and placenta may be the origin of some MSCs [8–11]. To date, this has not been confirmed in the mouse, and the ability to define and enrich this small subset using cell surface markers has not been demonstrated [12].

In addition to myocytes, osteocytes, and chondrocytes, under certain conditions, MSCs can differentiate into endodermal or neuroectodermal cell lineages including gastric epithelial cells (unpublished data), hepatocytes [13], pneumocytes [14], pigment epithelial cells [15] and astrocytes [16]. As a result, MSCs can effectively contribute to tissue repair [17]. MSC tissue repair may also occur independent of tissue engraftment or differentiation [17,18]. Moreover, MSCs may modulate the immune response. In the field of organ transplantation, MSCs have been shown to promote transplanted organ engraftment and reduce the cell immune-mediated graft-versus-host disease (GVHD) [19,20]. MSCs inhibit T-cell proliferation [21,22], induce T-cell apoptosis [23], and alter migratory property of T-cells [24]. The immune modulatory effect of MSCs has also been implicated in other chronic inflammatory diseases including autoimmune encephalomyelitis and hypoxic lung injury [25–29]. In the case of autoimmune enteropathy, it has been shown that MSCs can ameliorate inflammation independent of regulatory T cells [30].

Chronic inflammation is associated with increased risk of malignancy. In the gastrointestinal tract, examples include esophageal adenocarcinoma and Barrett's esophagus, gastric adenocarcinoma and *Helicobacter* infection, hepatocellular carcinoma and chronic viral hepatitis, and colorectal cancer and inflammatory bowel disease. Prolonged exposure to excessive proinflammatory activity has been regarded to foster tumorigenesis. In addition to the well-recognized Th1 lineage of CD4<sup>+</sup> T-helper cells, a growing body of literature has shown that a distinctive lineage of CD4<sup>+</sup> T cells, Th17 cells, may be important in inflammation and autoimmunity [31]. Th17 cells secrete interleukin (IL)-17A, IL-17F, IL-17A-IL-17F heterodimers, IL-21, and IL-22; these cells have been shown to be important for the clearance of extracellular pathogens. These Th17 cell responses are likely an early response mechanism for the clearance of such pathogens [32]. The mouse model of *Helicobacter felis* infection is a well-established model of gastritis and gastric cancer [33]. *Helicobacter* colonization of the murine stomach induces proinflammatory responses and promotes dysplastic changes and tumorigenesis approximately 10–12 months after infection. Moreover, it has previously been shown that IL-17 is overexpressed in *H. pylori*-infected gastric mucosa in both mice and humans [34–36]. In addition, IL-17<sup>-/-</sup> knockout mice have less severe inflammation when compared to wild-type mice [36]. However, the role of IL-17 in *Helicobacter*-induced gastric tumorigenesis is not well understood. Thus, the *H. felis* model of gastritis and gastric cancer

provides an excellent model in which the effects of MSCs and Th17 responses on inflammation-associated carcinogenesis can be studied.

In this study, we show that specific cell markers can be used to isolate bone marrow derived nonhematopoietic cells having characteristics of MSCs. Furthermore, using the murine *H. felis* model of gastritis and gastric dysplasia, we demonstrate that these freshly isolated cells may affect tumorigenesis by altering Th17-mediated responses.

## Materials and Methods

### Mice

All mice studies and breeding were carried out under the approval of Institutional Animal Care and Use Committee of Columbia University and Kaohsiung Medical University. Wild-type C57BL/6 female and male mice (6–8 weeks old), chicken  $\beta$ -actin enhanced green fluorescent protein (EGFP) transgenic male mice (6–8 weeks old), and UBC-GFP transgenic male mice (6–8 weeks old) were purchased from Jackson Laboratory (Bar Harbor, ME, <http://www.jax.org>) and National Laboratory Animal Center (Taipei, Taiwan). Mice were maintained in specific pathogen-free husbandry.

### Cell Isolation from the Bone Marrow, Peripheral Blood, and Spleen

Whole bone marrow cells were flushed from both femurs and tibias of mice with Hanks' balanced salt solution (HBSS) containing 5% fetal bovine serum (FBS; Gibco, Grand Island, NY, <http://www.invitrogen.com>). Cells from different donors were pooled together and filtered through a 40- $\mu$ m cell strainer (BD Biosciences, San Diego, CA, <http://www.bdbiosciences.com>). To obtain peripheral blood mononuclear cells, blood was drawn by percutaneous intracardiac puncture and mixed in acid citrate dextrose tubes (BD Biosciences) for anticoagulation. Red blood cells (RBC) were removed by RBC lysis buffer (BD Biosciences). To obtain splenocytes, spleens were ground on a 40- $\mu$ m cell strainer (BD Biosciences) and flushed with HBSS with 5% FBS (Gibco). Cell pellets were resuspended with HBSS containing 5% FBS following centrifugation (Gibco).

### Lineage Cell Depletion by Magnetic-Activated Cell Sorting

Whole bone marrow cells were resuspended with phosphate-buffered saline (PBS) containing 0.5% bovine serum albumin (BSA) and 2 mM EDTA (Miltenyi Biotec, Auburn, CA, <http://www.miltenyibiotec.com>) at a concentration of 10,000,000 cells per 10  $\mu$ L and incubated with Lineage depletion kit (Miltenyi Biotec), including a panel of biotinylated for CD5, CD45R (B220), CD11b, Anti-Gr-1 (Ly-6G/C), and Ter-119. Microbead-bound cells were further depleted by AutoMACS (Miltenyi Biotec) and the negative cell fraction was used for the majority of the experiments.

### Fluorescence-Activated Cell Sorting Analysis

Cells were diluted to a concentration of 1,000,000 cells per 100  $\mu$ L of HBSS with 5% FBS (Gibco) in 5 ml fluorescence-activated cell sorting (FACS) tubes (BD Biosciences). Antibodies used in this study were as follows: anti-mouse antibody of the Lineage cocktail-APC, CD45-PerCp-Cy5.5, CD44-PE, Sca1-PE-Cy7, Flk-1-PE, streptavidin-FITC, streptavidin-PE, streptavidin-APC, CD4-PE-Cy5, IL-17A-PE, FOXP3-Alexa647 (BD Pharmingen, San Diego, [http://www.bdbiosciences.com/index\\_us.shtml](http://www.bdbiosciences.com/index_us.shtml)), c-Kit-APC-Alexa 750, CD34-Alexa 700, CD44-Alexa700, SSEA1-PE, CD34-Biotin, CD90-Biotin, CD73-Biotin, and CD105-Biotin (eBioscience, San Diego, CA, <http://www.ebioscience.com/>). For intracellular cytokine staining, GolgiPlug (BD Biosciences, San Diego, CA, <http://www.ebiosciences.com>) was given for overnight incubation. Then 4',6-diamidino-2-phenylindole (DAKO, Glostrup,

Denmark, <http://www.dako.com>) was added at a concentration of 1/1,000 to exclude dead cells. FACS was performed on BD LSR and BD Aria cell sorters (BD Biosciences) and later analyzed on FlowJo 7.2 (FlowJo, Ashland, OR, <http://www.flowjo.com>).

### MSC Culture

Wild-type whole bone marrow cells were plated at a density of  $10^6$  cells/cm<sup>2</sup> in murine mesenchymal medium with murine mesenchymal supplements (MesenCult; Stem Cell Technologies, Vancouver, BC, Canada, <http://www.stemcell.com>). FACS-sorted cells derived from UBC-GFP transgenic mice were added to wells containing whole bone marrow cells as described above. Nonadherent cells were removed after 24 hours, and culture media changed every 5 days. Cells became confluent at approximately 3 weeks at 37°C in the humid air containing 5% CO<sub>2</sub>. MSCs were detached by 0.25% trypsin and 0.02% EDTA at 37°C for 2 min and subsequently passaged in the ratio of 1:3 to achieve the desired number.

### Fibroblastic Colony-Forming Unit Assay

Bone marrow cells were plated at a density of  $5 \times 10^5$  cells/cm<sup>2</sup> and maintained as described above. At day 14, using fluorescent microscope, we counted the green fluorescent protein (GFP) + fibroblastic colony-forming units (CFU-F), which was defined as a colony consisting of more than 100 cells.

### Differentiation Assays

To induce adipocyte differentiation, the subconfluent cells were cultured with MesenCult stem cell medium containing 5.0 µg/mL insulin, 50 µM indomethacin, 1 µM dexamethasone, and 0.5 µM 3-isobutyl-1-methylxanthine. After 14 days, these cells were fixed with 10% formalin for 20 minutes and stained with Oil Red-O. To induce osteocyte differentiation, the subconfluent cells were cultured with MesenCult stem cell medium containing 1 nM Dexamethasone, 20 mM β-glycerolphosphate, 50 µM L-ascorbic acid 2-phosphate sesquimagnesium salt, and 50 ng/mL L-thyroxine sodium pentahydrate. After 14 days, these cells were fixed with 10% formalin for 20 minutes, and characterization was performed by alizarin red staining, which detects calcium deposition.

### CD4+ T-Cell Activation

Mouse CD4+ T cells were isolated and negatively selected by microbeads (BD Pharmingen) from whole splenocytes. CD4+ T cells were activated by concanavalin A (conA) 5 µg/ml. Activation of CD4+ T cells was examined by MTS reaction (Promega, Madison, WI, <http://www.promega.com>). Bone marrow cells in study were cultured with CD4+ T cells in a ratio of 5:1 and 10:1 of CD4+ T cells to bone marrow cells. After 48 hours, cells were collected for FACS analysis (CD4, IL-17A, FOXP3), and culture supernatant collected for determination of cytokine (IL-6, IL-17A, IL-17F, IL-17AF) levels by enzyme-linked immunosorbent assay.

### Lethal Irradiation and Bone Marrow Transplantation

Using a Cs137 source irradiator, a total dose of 950 cGy irradiation was delivered in two sessions, 3 hours apart, to 8-week-old C57BL/6 wild-type female recipient mice. One hour after the final session of irradiation, 500,000 whole bone marrow cells from 8-week-old wild-type male mice plus 50,000 bone marrow-derived Lin<sup>-</sup>CD44<sup>hi</sup>Sca1<sup>-</sup>cKit<sup>+</sup>CD34<sup>-</sup> cells from 8-week-old chicken β-actin EGFP transgenic male mice (Jackson Laboratory) were infused by tail vein injection into recipient mice. In controls, only 500,000 whole bone marrow cells from either wild-type male donors or chicken β-actin EGFP transgenic male donors were transfused. All the recipient mice were maintained on neomycin-treated water (1.1 g/L) for 14 days immediately following irradiation.

## Inoculation of *H. Felis* and Infection COntirmation

A total of 15 study mice (age 3 months) were inoculated with *H. felis* by oral gavage, while 15 other mice remained uninfected. *H. felis* (ATCC 49179) was used for oral inoculation as described previously [17]. The organism was grown for 48 hours at 37°C under microaerobic conditions on 5% lysed horse blood agar. The bacteria were harvested and inoculated (at a titer of 1,010 organisms per milliliter) into brain heart infusion broth with 30% glycerol added. The bacterial suspension was frozen at -70°C. Prior to use, aliquots were thawed, analyzed for motility, and cultured for evidence of aerobic or anaerobic bacterial contamination. Brain heart infusion broth containing ~1,010 colony-forming units of *H. felis* per milliliter was used as inoculum. The inocula (0.5 ml) were delivered by gastric intubation into each test mouse three times at 2-day intervals by using a sterile oral catheter. After 1 year of infection, mice were euthanized. Both bone marrow and peripheral blood were extracted and used for MSC culture and mRNA detection.

## Results

### Bone Marrow Lin<sup>-</sup>CD44<sup>hi</sup>Sca1<sup>-</sup>cKit<sup>+</sup>CD34<sup>-</sup> Cells Are Effective in Producing CFU-F

To identify nonhematopoietic cells from murine bone marrow, we fractionated whole bone marrow by the cell surface markers, Lin (Lineage cocktail, including CD3ε, CD11b, CD45R/B220, Ly-76, Gr-1) and CD44<sup>+</sup> (supporting information Fig. 1). After removal of differentiated hematopoietic cells, Lin<sup>-</sup> typically denotes undifferentiated cells. CD44 is a cell surface marker that has consistently been shown to be a marker of MSCs both in vitro and in vivo [9]. We found that only Lin<sup>-</sup>CD44<sup>hi</sup> cells yield CFU-F, whereas Lin<sup>+</sup> and Lin<sup>-</sup>CD44<sup>lo</sup> do not generate any CFU-F (supporting information Fig. 2). To further exclude possible contamination by hematopoietic stem cells (HSC), previously defined as Lin<sup>-</sup>Sca1<sup>+</sup>cKit<sup>+</sup> [37], and common myeloid progenitors, previously defined as Lin<sup>-</sup>CD44<sup>hi</sup>Sca1<sup>-</sup>cKit<sup>+</sup>CD34<sup>+</sup> [38], we sorted cells according to their expression of Sca1, cKit, and CD34. We found that Lin<sup>-</sup>CD44<sup>hi</sup>Sca1<sup>-</sup>cKit<sup>+</sup>CD34<sup>-</sup> cells were just as effective as whole bone marrow in generating CFU-F (Fig. 1A). These results were confirmed in at least five separate experiments. Interestingly, freshly isolated Lin<sup>-</sup>CD44<sup>hi</sup>Sca1<sup>-</sup>cKit<sup>+</sup>CD34<sup>-</sup> cells rarely survived when cultured alone and required whole bone marrow cells to sustain in vitro cell proliferation. Using FACS analysis, we found that Lin<sup>-</sup>CD44<sup>hi</sup>Sca1<sup>-</sup>cKit<sup>+</sup>CD34<sup>-</sup> cells (Fig. 1B) made up only ~0.5%–1% of whole bone marrow cells and these cells were SSEA1<sup>-</sup>, Flk1<sup>-</sup>, CD90<sup>-</sup>, CD73<sup>-</sup>, and CD105<sup>+</sup> (27%) (Fig. 1C). The CFU-F efficiency of single Lin<sup>-</sup>CD44<sup>hi</sup>Sca1<sup>-</sup>cKit<sup>+</sup>CD34<sup>-</sup> cells was 21.3% (average 12.5 colonies out of 58.6 eligible wells; supporting information Fig. 3), whereas for single Lin<sup>-</sup>CD44<sup>hi</sup>Sca1<sup>-</sup>cKit<sup>-</sup> cells the CFU-F efficiency was only 7% (average 3.1 colonies out of 44.5 eligible wells, three separate experiments). Previous studies have shown that MSCs express Sca1, but not cKit [12]. Interestingly, in our study, we observed that Lin<sup>-</sup>CD44<sup>hi</sup>Sca1<sup>-</sup>cKit<sup>+</sup>CD34<sup>-</sup> cells gradually change their cell surface marker expression following in vitro culture and showed increased Sca1<sup>+</sup> expression and decreased cKit<sup>+</sup> expression after 14 days of in vitro culture (Fig. 1D). This cell population remained a constant proportion of murine bone marrow at 1 month and 28 months of life (supporting information Fig. 4). This suggests that these cells may be essential for preservation of bone marrow function.

### Bone Marrow Lin<sup>-</sup>CD44<sup>hi</sup>Sca1<sup>-</sup>cKit<sup>+</sup>CD34<sup>-</sup> Cells Engraft in the Bone Marrow and Give Rise to MSCs Following Bone Marrow Transplantation in Lethally Irradiated Recipient Mice

We transplanted 50,000 freshly isolated bone marrow-derived Lin<sup>-</sup>CD44<sup>hi</sup>Sca1<sup>-</sup>cKit<sup>+</sup>CD34<sup>-</sup> cells from syngeneic C57BL6 chicken β-actin EGFP male donors into lethally irradiated female recipient mice by tail vein infusion. In our initial three experiments, all recipient mice died within 4 weeks of transplantation, demonstrating the lack of short-term HSC potential of these donor cells (Table 1). In subsequent experiments, all



lethally irradiated recipient mice survived as we administered a radioprotective dose of wild-type whole bone marrow cells (~500,000 cells) and 50,000 freshly isolated GFP-labeled  $\text{Lin}^{-}\text{CD44}^{\text{hi}}\text{Sca1}^{-}\text{cKit}^{+}\text{CD34}^{-}$  cells (GFP-labeled bone marrow transplant [GFPL-BMT]) by tail vein injection. Although we did not detect any GFP-positive cells in the bone marrow using FACS, GFP-positive MSCs were recovered from whole bone marrow culture in 35% of GFPL-BMT recipients 4 and 8 months after transplantation (7 of 20 study mice; Fig. 2A, 2B). No GFP-positive MSCs were detected in control mice infused with wild-type whole bone marrow cells alone (Fig. 2C). After sorting by FACS, GFP-positive cells were passaged (Fig. 2D) and differentiated into osteoblasts (Fig. 2E) and adipocytes (Fig. 2F). However, we have not successfully differentiated our cells, or any other standard MSC, to chondrocytes due to technical problems. Nevertheless, the ability to differentiate these cells into adipocytes and osteocytes clearly demonstrates the multipotentiality of these bone marrow-derived cells. Furthermore, in bone marrow transplant experiments, GFP-positive cells were detected by immunohistochemistry in the tibia of GFPL-BMT mice (Fig. 2G), but not in mice transplanted with wild-type whole bone marrow alone (Fig. 2H). These GFP+  $\text{Lin}^{-}\text{CD44}^{\text{hi}}\text{Sca1}^{-}\text{cKit}^{+}\text{CD34}^{-}$  cells appeared spindle-shaped and were located near sinusoids (Fig. 2G), whereas GFP+ hematopoietic cells were found throughout the bone marrow (Fig. 2I).

### Bone Marrow $\text{Lin}^{-}\text{CD44}^{\text{hi}}\text{Sca1}^{-}\text{cKit}^{+}\text{CD34}^{-}$ Cells Reduce Th17 Differentiation

To determine whether  $\text{Lin}^{-}\text{CD44}^{\text{hi}}\text{Sca1}^{-}\text{cKit}^{+}\text{CD34}^{-}$  cells (abbreviated as L-44+) affect Th17 cell differentiation, we cocultured bone marrow cells with activated CD4+ T cells. CD4+ T cells were negatively selected from splenocytes of C57Bl6 syngeneic wild-type mice using microbeads and then activated by lectin protein ConA (5  $\mu\text{g}/\text{ml}$ ). Proliferation of CD4+ T cells was confirmed by the nonradioactive cell proliferation assay using 3-(4,5-dimethylthiazol-2-yl)-5-(3-carboxymethoxyphenyl)-2-(4-sulfophenyl)-2H-tetrazolium; MTS, data not shown). Whole bone marrow cells and bone marrow-derived  $\text{Lin}^{-}\text{CD44}^{\text{lo}}$  cells (abbreviated as L-44-) were used as additional controls. L-44- cells are undifferentiated cells that, unlike L-44+ cells, do not possess the ability to generate CFU-F. When cocultured at a ratio of 10:1 (activated CD4+ T cells: bone marrow cells) for 48 hours, the percentage of CD4+IL-17+ cells was significantly reduced in the L-44+ cocultured cells compared to whole bone marrow cocultured cells (Fig. 3A); CD4+ T-cell control vs. whole bone marrow vs. L-44+, 0.4% vs. 1.3% vs. 0.1% respectively;  $p < .05$ ). A comparable result using L-44- cells was only attainable with a much higher concentration of cells (5:1, Fig. 3A). Cytokine levels of IL-17A, IL-17F and IL-17A-F in culture supernatants were also lower in the L-44+ cell group than in activated CD4+ T-cell controls (supporting information Fig. 5). Correspondingly, increased expression of the transcription factor FOXP3, an inhibitor of Th17 differentiation, and decreased levels of IL-6, a known inducer of Th17 differentiation [39], were found in the L-44+ cell treated cultures (Fig. 3B, 3C;  $p < .05$ ) [40].

### Bone Marrow-Derived $\text{Lin}^{-}\text{CD44}^{\text{hi}}\text{Sca1}^{-}\text{cKit}^{+}\text{CD34}^{-}$ Cells Traffic to the Bone Marrow and Are Detectable in the Circulation Following Infusion into Nonirradiated Mice

To further evaluate the function of freshly isolated bone marrow  $\text{Lin}^{-}\text{CD44}^{\text{hi}}\text{Sca1}^{+}\text{cKit}^{+}\text{CD34}^{-}$  cells, we infused 50,000 cells into nonirradiated mice by tail vein injection. Although some infused cells trafficked to the gastric mucosa and submucosa (Fig. 4A–4C), the vast majority of the infused cells tracked to the bone marrow (0.1% of 100,000 bone marrow cells), spleen (0.3% of 50,000 splenocytes), and peripheral blood (0.2% of 10,000 peripheral blood mononuclear cells; Fig. 4D–4F). These cells were not trapped within the lung, and the number of GFP-positive cells detectable in the various organs above gradually declined within 2 weeks after infusion. However, few of the infused cells that lodged in the bone marrow survived after three passages of MSC culture (Fig. 4G, 4H). Infused cells found in the spleen, blood, and gastric tissue could not be propagated.

## Repeated Infusions of Bone Marrow-Derived Lin<sup>-</sup>CD44<sup>hi</sup>Sca1<sup>-</sup>cKit<sup>+</sup>CD34<sup>-</sup> Cells Reduce Progression to Low-Grade Gastric Dysplasia in Association with Decreased Th17 Cytokines

To confirm our in vitro findings of decreased Th17 cells by Lin<sup>-</sup>CD44<sup>hi</sup>Sca1<sup>-</sup>cKit<sup>+</sup>CD34<sup>-</sup> cells, we performed in vivo studies examining the effects of bone marrow cell infusion in mice with chronic *H. felis* infection. In preliminary experiments, increased IL-17A, not interferon (IFN)- $\gamma$ , was associated with progression from chronic gastritis to low-grade gastric dysplasia 4 months after a single infusion of 5,000,000 whole bone marrow cells into mice with chronic *H. felis* infection (dysplasia score, *H. felis* infection control vs. single infusion, 0.1 vs. 1.5;  $n = 10$  mice per group;  $p < .001$ ; supporting information Fig. 6B, 6C). Significant infiltration of both mononuclear and polymorphonuclear cells was observed in association with accelerated low-grade gastric dysplasia (supporting information 6A). In addition, we observed increased serum IL-17A levels (supporting information 6C,  $p < .05$ ) and increased IL-17A and IL-17F gastric tissue gene expression (supporting information 6D,  $p < .05$ ) in association with progression of chronic gastritis to low-grade gastric dysplasia. These data suggest that Th17 cytokines correlate with gastric tumorigenesis.

To investigate whether bone marrow-derived Lin<sup>-</sup>CD44<sup>hi</sup>Sca1<sup>-</sup>cKit<sup>+</sup>CD34<sup>-</sup> cells (L-44+ cells) can affect development of low-grade dysplasia, we further infused 50,000 L-44+ cells once per month for 4 consecutive months in mice with low-grade gastric dysplasia 10 months following *H. felis* infection (average dysplasia score = 1.0 in five *H. felis* infection control mice). *H. felis*-infected mice infused with 5,000,000 whole bone marrow cells served as controls. Following four L-44+ cell infusions, no dysplasia was detectable in 60% (3 of 5) of L-44+ cell treated mice (Fig. 5A, 5B), whereas 100% dysplasia was detected in *H. felis*-infected control mice (5 of 5, average dysplasia score = 1.0), 100% dysplasia detected in whole bone marrow-treated mice (5 of 5, average dysplasia score = 1.5), and no dysplasia present in *H. felis*-uninfected control mice (4 of 4; chi-square test,  $p .038$ ).

To rule out a bacterial load-related effect on dysplasia, we confirmed that an equivalent bacterial load, as determined by quantitative polymerase chain reaction (Fig. 5C), was administered to all groups. Notably, the gene expression of IL-17F, IL-22, and ROR- $\gamma$ t was reduced in the gastric tissue of L-44+ cell-infused mice, compared to *H. felis*-infected control mice ( $p < .05$ ) (Fig. 6). Previous literature has suggested that IL-17A and IL-17F levels generally parallel each other in vivo. In our study, although IL-17A levels were not significantly reduced in the L-44+ cell-infused group, when we divided the L-44+-treated group among those mice that responded to the cell infusion (i.e., had complete absence of dysplasia) versus those that did not (i.e., progressed to dysplasia), IL-17A levels remained significantly elevated in the two nonresponding mice, whereas a significant reduction in IL-17A levels was noted in the three responding mice (data not shown). These results suggest that Th17-associated cytokines and transcription factors may be important in the progression from chronic gastritis to low-grade gastric dysplasia. Multiple infusions of bone marrow Lin<sup>-</sup>CD44<sup>hi</sup>Sca1<sup>-</sup>cKit<sup>+</sup>CD34<sup>-</sup> cells may reduce Th17-associated responses and delay this progression.

## Discussion

Recent studies have suggested that human CD146<sup>+</sup> pericytes may be the origin of some MSCs in peripheral tissues. These cells have been shown to play an important role in tissue homeostasis [41]. However, it is not known whether bone marrow-derived MSCs may also contribute to this process. In an attempt to identify and isolate MSCs in vivo, we have shown that FACS-isolated bone marrow Lin<sup>-</sup>CD44<sup>hi</sup>Sca1<sup>-</sup>cKit<sup>+</sup>CD34<sup>-</sup> cells (L-44+ cells) contribute to a population of cells with CFU-F forming ability. These L-44+ cells have several characteristics of MSCs, including CFU-F ability and long-term engraftment following bone marrow transplantation. Recently, Wong et al. reported that a cellular subset of mouse bone

marrow derived cells was capable of myo-remodeling, but this cell population was sorted based on the cell surface marker Lin and CD45 [42]. The most significant difference from our findings was the further isolation of our bone marrow-derived cells using CD44. We chose CD44 as a cell selection tool because this marker has consistently been shown to be expressed in human MSCs in vivo and in vitro, and is also expressed in mouse MSCs (our unpublished data). More importantly, we showed that high expression of CD44 is closely related to CFU-F forming ability, a prerequisite for the isolation of MSCs. In addition to CFU-F, bone marrow-derived L-44+ cells can differentiate into osteoblasts and adipocytes. Nevertheless, similar to previously described MSCs, these L-44+ cells do engraft in the bone marrow as spindle-shaped and perisinusoidal cells, resemble pericytes with respect to their native tissue location, and can give rise to CFU-F. Based on the CFU-F efficiency of single L-44+ cells, we found that only ~21% of these L-44+ cells possess the ability to give rise to CFU-F cells. Thus, our data suggest that these cells are still a heterogenous population in which only a select percentage of cells are likely the bona fide MSCs.

Our findings demonstrate that there is a dynamic change in cell surface marker expression upon culturing of these CFU-F cells. Bone marrow-derived Lin<sup>-</sup>CD44<sup>hi</sup>Sca1<sup>-</sup>cKit<sup>+</sup>CD34<sup>-</sup> cells (L-44+ cells) gradually increased Sca1 and decreased cKit expression after culture of these cells in vitro. This process occurred as early as 14 days after plating, at a time when these cells begin to form CFU-F. These findings may explain why several groups have previously reported that bone marrow-derived MSCs are Sca1<sup>+</sup> and cKit<sup>-</sup> following their isolation and in vitro culture. Notably, our results demonstrate the importance of the cell surface marker cKit, as this marker is generally not expressed on MSCs in vitro. We demonstrate that the cKit<sup>+</sup> cell population can further enrich CFU-F ability and that L-44+ cells change their cell surface marker expression upon removal from their bone marrow niche, thus proving why it is difficult to identify these cells after mobilization into the circulation.

We previously showed that increased numbers of MSCs are detectable in the peripheral blood of mice following chronic *H. felis* infection (unpublished data). Given that MSCs have immune-modulating effects, we hypothesized that these cells may affect inflammation-associated tumorigenesis. To test this hypothesis, we infused Lin<sup>-</sup>CD44<sup>hi</sup>Sca1<sup>-</sup>cKit<sup>+</sup>CD34<sup>-</sup> cells (L-44+ cells) into nonirradiated *H. felis*-infected mice. After infusing into nonirradiated *H. felis*-infected mice, most of the L-44+ cells homed to the bone marrow, while small subsets of cells were detectable in spleen, peripheral blood, and stomach, including both the gastric mucosa and submucosa. The number of these GFP+ cells in the stomach was small, and long-term engraftment (i.e., greater than 2 weeks) was not seen here or elsewhere. It is likely that there was no bone marrow niche available for the infused cells in nonirradiated mice. Given their short-term survival in nonirradiated animals, a minimum threshold number of cells may be required for their anti-inflammatory or antitumorigenic effects to be detectable. Thus, to magnify possible effects, we administered multiple infusions of L-44+ cells into nonirradiated *H. felis*-infected mice. Indeed, the finding of delayed immune-mediated histopathologic progression in the stomach, in the absence of long-term engraftment of EGFP+ cells, suggests that the cellular infusions resulted in prolonged and systemic alterations in the *Helicobacter*-dependent immune response. Systemic cytokine levels were significantly affected by repeated (4 infusions over 4 months) L-44+ cell treatments. The development of gastric dysplasia in the *Helicobacter* mouse model has been shown to be largely dependent on the polarization and intensity of the immune response to the bacteria, and given the correlation between the reduced Th17 responses and delayed progression to dysplasia, this suggests that the effects of L-44+ cells may be related to this reprogramming of the immune response. Moreover, we believe that L-44+ cells may also be acting at peripheral sites such as the spleen, lymph nodes, or bone marrow. It is clear from studies performed by our group and others that the immune response to *H. felis* can be modulated by extragastric effects [43]. For example, infection of mice with *H. polygyrus*, a Helminth that colonizes the intestinal mucosa for mice for only 4–6 weeks can



inhibit proinflammatory responses to *H. felis* for many months. Thus, we propose that infusion of L-44+ cells can modulate the systemic cytokine changes that occur in response to *H. felis* infection.

Lin<sup>-</sup>CD44<sup>hi</sup>Sca1<sup>-</sup>cKit<sup>+</sup>CD34<sup>-</sup> cells (L-44+ cells) reduced progression of gastric dysplasia. In nonirradiated mice, whole bone marrow cells comprised mainly of hematopoietic cells, invoked robust inflammation, and even promoted dysplastic changes. In contrast, bone marrow-derived L-44+ cells did not have this effect. In addition, whole bone marrow cells induced Th17 proinflammatory cytokines (IL-17F, IL-22), whereas L-44+ cells suppressed these cytokines. We observed a significant reduction in IL-17F levels, while there was a trend toward reduced IL-17A levels that did not reach statistical significance. Interestingly, we detected increased IL-17A in the serum of whole bone marrow cell infused mice, whereas this was significantly reduced in L-44+ cell infused mice. Thus, another possibility is that the tissue response lags behind the cytokine changes. Although it is conceivable that IL-17A and IL-17F may have different functions in different organs and diseases, in general, IL-17A and IL-17F appear to change in parallel in vivo [44,45]. This is supported by our study, in which we observed greater reductions in IL-17F gene expression after L-44+ cell infusions, but also a better correlation between levels of IL-17A and the degree of dysplasia in our mice. That is, IL-17A levels remained significantly elevated in two mice that did not respond to L-44+ cell infusion (i.e., progressed to dysplasia), whereas a significant reduction in IL-17A levels was noted in the three mice that did respond (i.e., had absence of dysplasia). Therefore, L-44+ cells identify a population of CFU-F cells with immune modulatory effects on regulation of Th17 cell differentiation.

In cellular immunity, IFN- $\gamma$ , a T-helper type 1 (Th1) cell cytokine, is recognized to be important [46]. More recently, the traditional Th1 and Th2 dichotomy has been challenged by the finding of Th17 cell involvement in autoimmunity and cell-mediated immunity [47]. Th17 cells are characterized by the production of IL-17A, IL-17F, and IL-22, and are involved in the elimination of extracellular pathogens not cleared by Th1 or Th2 mediated pathways [32]. In *Helicobacter*-associated conditions, most of the focus in the past has been on mainly on Th1 cytokines. Colonization of the mammalian stomach induces proinflammatory responses that are largely responsible for the progression of tumorigenesis. We and others have previously demonstrated that inhibition of histopathologic progression to dysplasia is governed predominantly by this proinflammatory response [48,49]. Furthermore, Th17 cells have been implicated in these conditions and IL-17 expression is increased in *H. pylori*-infected gastric mucosa [50–53]. It has also been shown that IL-17A promoter polymorphism (rs2275913) is significantly associated with intestinal type of gastric cancer [54], while IL-17F polymorphism (rs763780) is associated with functional dyspepsia [55]. Nevertheless, the role of the Th17 immune response in *Helicobacter*-dependent gastric cancer has not yet been clearly addressed [33].

Although our data are somewhat limited by the small numbers of mice, we found the results extremely encouraging. In terms of the nonresponders, there was some degree of biological variability in this murine model that cannot in each case be accounted for. Although the mice are inbred and in theory genetically identical and received the same inoculum of *H. felis*, they do not always respond and progress in identical fashion. However, the complete absence of dysplasia in 60% of the mice is in our experience significant and without precedent. In the current study, we clearly demonstrate the anti-inflammatory effects of the Lin<sup>-</sup>CD44<sup>hi</sup>Sca1<sup>-</sup>cKit<sup>+</sup>CD34<sup>-</sup> cells and show good correlation between downregulation of Th17 responses and inhibition of progression to dysplasia. Although correlation may not necessarily indicate causation, our data is consistent with previous literature implicating an important role for Th17 cytokines in *Helicobacter*-induced immune responses [50–53].

In correlation with the *in vivo* data, we showed that *in vitro* coculture of CD4<sup>+</sup> T-cells with Lin<sup>-</sup>CD44<sup>hi</sup>Sca1<sup>-</sup>cKit<sup>+</sup>CD34<sup>-</sup> cells (L-44<sup>+</sup> cells), in contrast to whole bone marrow, did not increase the number of CD4<sup>+</sup>IL-17<sup>+</sup> cells detectable by FACS. Furthermore, whole bone marrow increased IL-17 cytokines in coculture supernatant, whereas L-44<sup>+</sup> cells did not. Thus, our *in vitro* and *in vivo* data suggests that the most significant effect of bone marrow-derived L-44<sup>+</sup> cells may be to reduce Th17 cell differentiation. To date, the association between MSCs and Treg or Th17 cells is still not clearly understood and needs further investigation [20,56, 57].

In summary, our combination of cell surface markers, Lin<sup>-</sup>CD44<sup>hi</sup>Sca1<sup>-</sup>cKit<sup>+</sup>CD34<sup>-</sup>, can be used to identify a non-hematopoietic cell population with characteristics of MSCs. In nonirradiated mice, whole bone marrow infusion accelerates dysplasia in a *H. felis* murine model of gastric cancer, whereas Lin<sup>-</sup>CD44<sup>hi</sup>Sca1<sup>-</sup>cKit<sup>+</sup>CD34<sup>-</sup> cell infusion does not. The inhibition of Th17 cells by Lin<sup>-</sup>CD44<sup>hi</sup>Sca1<sup>-</sup>cKit<sup>+</sup>CD34<sup>-</sup> cells is associated with this reduced dysplasia in chronic *H. felis* infection. Nevertheless, additional studies examining the interaction between bone marrow-derived non-hematopoietic cells and Th17 cells are needed to further characterize the role of the immune response in gastric tumorigenesis.

## Supplementary Material

Refer to Web version on PubMed Central for supplementary material.

## Acknowledgments

The authors thank Dr. Yu-Chun Lin and Chia-Jung Lee in Kaohsiung Medical University Hospital for their technical support. This work was supported by the National Institutes of Health (5R01 CA120979-02). Samuel Asfaha is supported by a fellowship from the Canadian Institute of Health Research and Albert Heritage Foundation for Medic Research.

## References

1. Kuo TK, Hung SP, Chuang CH, et al. Stem cell therapy for liver disease: parameters governing the success of using bone marrow mesenchymal stem cells. *Gastroenterology* 2008;134:2111–2113. [PubMed: 18455168]
2. Le Blanc K, Ringden O. Mesenchymal stem cells: properties and role in clinical bone marrow transplantation. *Curr Opin Immunol* 2006;18:586–591. [PubMed: 16879957]
3. Prockop DJ. Marrow stromal cells as stem cells for nonhematopoietic tissues. *Science* 1997;276:71–74. [PubMed: 9082988]
4. Caplan AI. Mesenchymal stem cells. *J Orthop Res* 1991;9:641–650. [PubMed: 1870029]
5. Owen M, Friedenstein AJ. Stromal stem cells: marrow-derived osteogenic precursors. *Ciba Found Symp* 1988;136:42–60. [PubMed: 3068016]
6. Pittenger MF, Mackay AM, Beck SC, et al. Multilineage potential of adult human mesenchymal stem cells. *Science* 1999;284:143–147. [PubMed: 10102814]
7. Dominici M, Le Blanc K, Mueller I, et al. Minimal criteria for defining multipotent mesenchymal stromal cells. The International Society For Cellular Therapy Position Statement. *Cytotherapy* 2006;8:315–317. [PubMed: 16923606]
8. Caplan AI. All MSCs are pericytes? *Cell Stem Cell* 2008;3:229–230. [PubMed: 18786406]
9. Crisan M, Yap S, Casteilla L, et al. A perivascular origin for mesenchymal stem cells in multiple human organs. *Cell Stem Cell* 2008;3:301–313. [PubMed: 18786417]
10. Dellavalle A, Sampaolesi M, Tonlorenzi R, et al. Pericytes of human skeletal muscle are myogenic precursors distinct from satellite cells. *Nat Cell Biol* 2007;9:255–267. [PubMed: 17293855]
11. Sacchetti B, Funari A, Michienzi S, et al. Self-renewing osteoprogenitors in bone marrow sinusoids can organize a hematopoietic microenvironment. *Cell* 2007;131:324–336. [PubMed: 17956733]

12. Holmes C, Stanford WL. Concise review: stem cell antigen-1: expression, function, and enigma. *Stem Cells* 2007;25:1339–1347. [PubMed: 17379763]
13. Lee KD, Kuo TK, Whang-Peng J, et al. In vitro hepatic differentiation of human mesenchymal stem cells. *Hepatology* 2004;40:1275–1284. [PubMed: 15562440]
14. Ortiz LA, Gambelli F, McBride C, et al. Mesenchymal stem cell engraftment in lung is enhanced in response to bleomycin exposure and ameliorates its fibrotic effects. *Proc Natl Acad Sci USA* 2003;100:8407–8411. [PubMed: 12815096]
15. Arnholt S, Heiduschka P, Klein H, et al. Adenovirally transduced bone marrow stromal cells differentiate into pigment epithelial cells and induce rescue effects in RCS rats. *Invest Ophthalmol Vis Sci* 2006;47:4121–4129. [PubMed: 16936132]
16. Kopen GC, Prockop DJ, Phinney DG. Marrow stromal cells migrate throughout forebrain and cerebellum, and they differentiate into astrocytes after injection into neonatal mouse brains. *Proc Natl Acad Sci USA* 1999;96:10711–10716. [PubMed: 10485891]
17. Phinney DG, Prockop DJ. Concise review: mesenchymal stem/multipotent stromal cells: the state of transdifferentiation and modes of tissue repair—current views. *Stem Cells* 2007;25:2896–2902. [PubMed: 17901396]
18. Prockop DJ. “Stemness” does not explain the repair of many tissues by mesenchymal stem/multipotent stromal cells (MSCs). *Clin Pharmacol Ther* 2007;82:241–243. [PubMed: 17700588]
19. Karlsson H, Samarasinghe S, Ball LM, et al. Mesenchymal stem cells exert differential effects on alloantigen and virus-specific T-cell responses. *Blood* 2008;112:532–541. [PubMed: 18445691]
20. Aggarwal S, Pittenger MF. Human mesenchymal stem cells modulate allogeneic immune cell responses. *Blood* 2005;105:1815–1822. [PubMed: 15494428]
21. Ren G, Zhang L, Zhao X, et al. Mesenchymal stem cell-mediated immunosuppression occurs via concerted action of chemokines and nitric oxide. *Cell Stem Cell* 2008;2:141–150. [PubMed: 18371435]
22. Ramasamy R, Tong CK, Seow HF, et al. The immunosuppressive effects of human bone marrow-derived mesenchymal stem cells target T cell proliferation but not its effector function. *Cell Immunol* 2008;251:131–136. [PubMed: 18502411]
23. Plumas J, Chaperot L, Richard MJ, et al. Mesenchymal stem cells induce apoptosis of activated T cells. *Leukemia* 2005;19:1597–1604. [PubMed: 16049516]
24. Li H, Guo Z, Jiang X, et al. Mesenchymal stem cells alter migratory property of T and dendritic cells to delay the development of murine lethal acute graft-versus-host disease. *Stem Cells* 2008;26:2531–2541. [PubMed: 18635870]
25. El-Badri NS, Hakki A, Ferrari A, et al. Autoimmune disease: is it a disorder of the microenvironment? *Immunol Res* 2008;41:79–86. [PubMed: 18506645]
26. Kassis I, Grigoriadis N, Gowda-Kurkalli B, et al. Neuroprotection and immunomodulation with mesenchymal stem cells in chronic experimental autoimmune encephalomyelitis. *Arch Neurol* 2008;65:753–761. [PubMed: 18541795]
27. Ortiz LA, Dutreil M, Fattman C, et al. Interleukin 1 receptor antagonist mediates the antiinflammatory and antifibrotic effect of mesenchymal stem cells during lung injury. *Proc Natl Acad Sci USA* 2007;104:11002–11007. [PubMed: 17569781]
28. Patel KM, Crisostomo P, Lahm T, et al. Mesenchymal stem cells attenuate hypoxic pulmonary vasoconstriction by a paracrine mechanism. *J Surg Res* 2007;143:281–285. [PubMed: 17868699]
29. Uccelli A, Moretta L, Pistoia V. Mesenchymal stem cells in health and disease. *Nat Rev Immunol* 2008;8:726–736. [PubMed: 19172693]
30. Parekkadan B, Tilles AW, Yarmush ML. Bone marrow-derived mesenchymal stem cells ameliorate autoimmune enteropathy independently of regulatory T cells. *Stem Cells* 2008;26:1913–1919. [PubMed: 18420833]
31. Park H, Li Z, Yang XO, et al. A distinct lineage of CD4 T cells regulates tissue inflammation by producing interleukin 17. *Nat Immunol* 2005;6:1133–1141. [PubMed: 16200068]
32. Bettelli E, Korn T, Oukka M, et al. Induction and effector functions of T(H)17 cells. *Nature* 2008;453:1051–1057. [PubMed: 18563156]
33. Fox JG, Wang TC. Inflammation, atrophy, and gastric cancer. *J Clin Invest* 2007;117:60–69. [PubMed: 17200707]

34. Lizza F, Parrello T, Monteleone G, et al. Up-regulation of IL-17 is associated with bioactive IL-8 expression in *Helicobacter pylori*-infected human gastric mucosa. *J Immunol* 2000;165:5332–5337. [PubMed: 11046068]
35. Algood HM, Gallo-Romero J, Wilson KT, et al. Host response to *Helicobacter pylori* infection before initiation of the adaptive immune response. *Fems Immunol Med Microbiol* 2007;51:577–586. [PubMed: 17919297]
36. Shiomi S, Toriie A, Imamura S, et al. IL-17 is involved in *Helicobacter pylori*-induced gastric inflammatory responses in a mouse model. *Helicobacter* 2008;13:518–524. [PubMed: 19166417]
37. Morrison SJ, Weissman IL. The long-term repopulating subset of hematopoietic stem cells is deterministic and isolatable by phenotype. *Immunity* 1994;1:661–673. [PubMed: 7541305]
38. Akashi K, Traver D, Miyamoto T, et al. A clonogenic common myeloid progenitor that gives rise to all myeloid lineages. *Nature* 2000;404:193–197. [PubMed: 10724173]
39. Bettelli E, Carrier Y, Gao W, et al. Reciprocal developmental pathways for the generation of pathogenic effector TH17 and regulatory T cells. *Nature* 2006;441:235–238. [PubMed: 16648838]
40. Zhou L, Lopes JE, Chong MM, et al. TGF-beta-induced Foxp3 inhibits T(H)17 cell differentiation by antagonizing RORgamma function. *Nature* 2008;453:236–240. [PubMed: 18368049]
41. Valtieri M, Sorrentino A. The mesenchymal stromal cell contribution to homeostasis. *J Cell Physiol* 2008;217:296–300. [PubMed: 18615579]
42. Wong SH, Lowes KN, Bertoncello I, et al. Evaluation of Sca-1 and c-Kit as selective markers for muscle remodelling by nonhemopoietic bone marrow cells. *Stem Cells* 2007;25:1364–1374. [PubMed: 17303817]
43. Fox JG, Beck P, Dangler CA, et al. Concurrent enteric helminth infection modulates inflammation and gastric immune responses and reduces *helicobacter*-induced gastric atrophy. *Nat Med* 2000;6:536–542. [PubMed: 10802709]
44. Tan W, Huang W, Gu X, et al. IL-17F/IL-17R interaction stimulates granulopoiesis in mice. *Exp Hematol* 2008;36:1417–1427. [PubMed: 18723265]
45. Toy D, Kugler D, Wolfson M, et al. Cutting edge: interleukin 17 signals through a heteromeric receptor complex. *J Immunol* 2006;177:36–39. [PubMed: 16785495]
46. Steinman L. A brief history of T(H)17, the first major revision in the T(H)1/T(H)2 hypothesis of T cell-mediated tissue damage. *Nat Med* 2007;13:139–145. [PubMed: 17290272]
47. Ferber IA, Brocke S, Taylor-Edwards C, et al. Mice with a disrupted IFN-gamma gene are susceptible to the induction of experimental autoimmune encephalomyelitis (EAE). *J Immunol* 1996;156:5–7. [PubMed: 8598493]
48. Eaton KA, Mefford M, Thevenot T. The role of T cell subsets and cytokines in the pathogenesis of *Helicobacter pylori* gastritis in mice. *J Immunol* 2001;166:7456–7461. [PubMed: 11390498]
49. Eaton KA, Ringler SR, Danon SJ. Murine splenocytes induce severe gastritis and delayed-type hypersensitivity and suppress bacterial colonization in *Helicobacter pylori*-infected SCID mice. *Infect Immun* 1999;67:4594–4602. [PubMed: 10456905]
50. Caruso R, Pallone F, Monteleone G. Emerging role of IL-23/IL-17 axis in *H pylori*-associated pathology. *World J Gastroenterol* 2007;13:5547–5551. [PubMed: 17948927]
51. Mizuno T, Ando T, Nobata K, et al. Interleukin-17 levels in *Helicobacter pylori*-infected gastric mucosa and pathologic sequelae of colonization. *World J Gastroenterol* 2005;11:6305–6311. [PubMed: 16419159]
52. Lizza F, Parrello T, Sebkova L, et al. Expression of proinflammatory and Th1 but not Th2 cytokines is enhanced in gastric mucosa of *Helicobacter pylori* infected children. *Dig Liver Dis* 2001;33:14–20. [PubMed: 11303969]
53. Kullberg MC, Jankovic D, Feng CG, et al. IL-23 plays a key role in *Helicobacter hepaticus*-induced T cell-dependent colitis. *J Exp Med* 2006;203:2485–2494. [PubMed: 17030948]
54. Shibata T, Tahara T, Hirata I, et al. Genetic polymorphism of interleukin-17A and -17F genes in gastric carcinogenesis. *Hum Immunol* 2009;70:547–551. [PubMed: 19414056]
55. Arisawa T, Tahara T, Shibata T, et al. Genetic polymorphisms of molecules associated with inflammation and immune response in Japanese subjects with functional dyspepsia. *Int J Mol Med* 2007;20:717–723. [PubMed: 17912466]

56. Prevosto C, Zancolli M, Canevali P, et al. Generation of CD4+ or CD8+ regulatory T cells upon mesenchymal stem cell-lymphocyte interaction. *Haematologica* 2007;92:881–888. [PubMed: 17606437]
57. Jones BJ, McTaggart SJ. Immunosuppression by mesenchymal stromal cells: from culture to clinic. *Exp Hematol* 2008;36:733–741. [PubMed: 18474304]



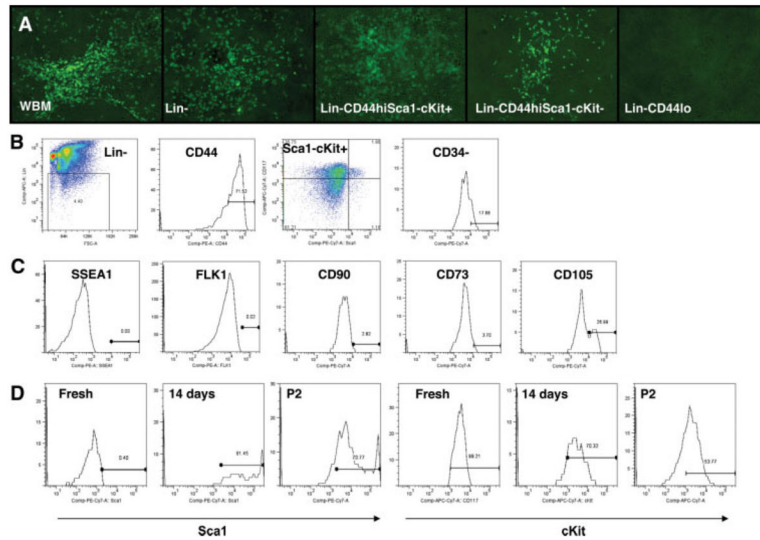


**Figure 1.**

Bone marrow-derived  $\text{Lin}^- \text{CD44}^{\text{hi}} \text{Sca1}^- \text{cKit}^+$  cells can yield as many fibroblastic colony-forming units (CFU-F) as whole bone marrow cells. **(A):** We fractionated the whole bone marrow according to their cell surface markers. Here we show five groups: (1) whole bone marrow, (2)  $\text{Lin}^-$ , (3)  $\text{Lin}^- \text{CD44}^{\text{hi}} \text{Sca1}^- \text{cKit}^+$ , (4)  $\text{Lin}^- \text{CD44}^{\text{hi}} \text{Sca1}^- \text{cKit}^-$ , and (5)  $\text{Lin}^- \text{CD44}^{\text{lo}}$ . GFP-labeled CFU-F derived from  $\text{Lin}^- \text{CD44}^{\text{hi}} \text{Sca1}^- \text{cKit}^+$  cells were comparable to WBM (100 $\times$ ). **(B):** Gating strategy for fluorescence-activated cell sorting. We started from lineage negative cells from whole bone marrow, and then sorted for CD44. In the  $\text{Lin}^- \text{CD44}^{\text{hi}}$  subset, 35%–40% of cells were  $\text{Sca1}^- \text{cKit}^+$  (left upper quadrant). In the  $\text{Lin}^- \text{CD44}^{\text{hi}} \text{Sca1}^- \text{cKit}^+$  subset, 20% of cells were  $\text{CD34}^+$ . **(C):**  $\text{Lin}^- \text{CD44}^{\text{hi}} \text{Sca1}^- \text{cKit}^+ \text{CD34}^-$  cells were  $\text{SSEA1}^-$ ,  $\text{Flk}^-$ ,  $\text{CD90}^-$ , and  $\text{CD73}^-$  and 27% of cells were  $\text{CD105}^+$  (average data from 5 mice). **(D):** Expression of  $\text{Sca1}$  and  $\text{cKit}$  in CFU-F derived from  $\text{Lin}^- \text{CD44}^{\text{hi}} \text{Sca1}^- \text{cKit}^+ \text{CD34}^-$  cells culture.  $\text{Sca1}^+$  was highly expressed as early as 14 days after plating and persisted, at least after two passages, while  $\text{cKit}$  was gradually reduced during culture.

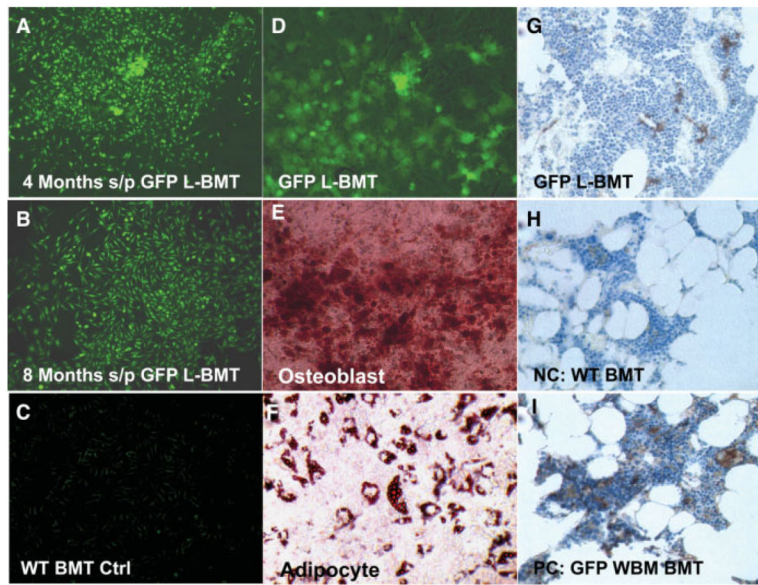


**Figure 2.**

Bone marrow-derived  $\text{Lin}^- \text{CD44}^{\text{hi}} \text{Sca1}^- \text{cKit}^+ \text{CD34}^-$  cells can engraft in the bone marrow of lethally irradiated hosts in the long term. **(A, B)**: Green fluorescent protein (GFP)-positive fibroblastic colony-forming units (CFU-F) derived from the lethally irradiated recipient mice transplanted with GFP+  $\text{Lin}^- \text{CD44}^{\text{hi}} \text{Sca1}^- \text{cKit}^+ \text{CD34}^-$  cells (L-BMT) 4 months **(A)** and 8 months **(B)** after transplantation (100 $\times$ ). **(C)**: No GFP+ CFU-F was obtained from mice transplanted with wild-type whole bone marrow cells transplantation (100 $\times$ ). **(D)**: GFP+ mesenchymal stem cells (MSCs) derived from L-BMT CFU-F (passage 3 is shown, 100 $\times$ ). **(E)**: GFP+ MSCs derived L-BMT from were purified by fluorescence-activated cell sorting (FACS) and differentiated to osteoblasts (stained by Alizarin Red, 100 $\times$ ). **(F)**: GFP+ MSCs derived from L-BMT were purified by FACS and differentiated to adipocytes (stained by Oil Red O, 100 $\times$ ). **(G)**: Donor-derived GFP+ cells appeared spindle-shaped and were mostly located in perisinusoidal areas within the marrow of recipient mice 8 months after bone marrow transplantation (400 $\times$ ). **(H)**: No GFP+ cells were found in the bone marrow of mice receiving wild-type whole bone marrow cells (400 $\times$ ). **(I)**: Most of the GFP+ cells are hematopoietic cells in the bone marrow of mice receiving GFP+ whole bone marrow cells 8 months after bone marrow transplantation (400 $\times$ ). **(G–I)**: Formalin-fixed paraffin embedded sections of bone marrow, 5  $\mu\text{m}$ , anti-GFP staining.

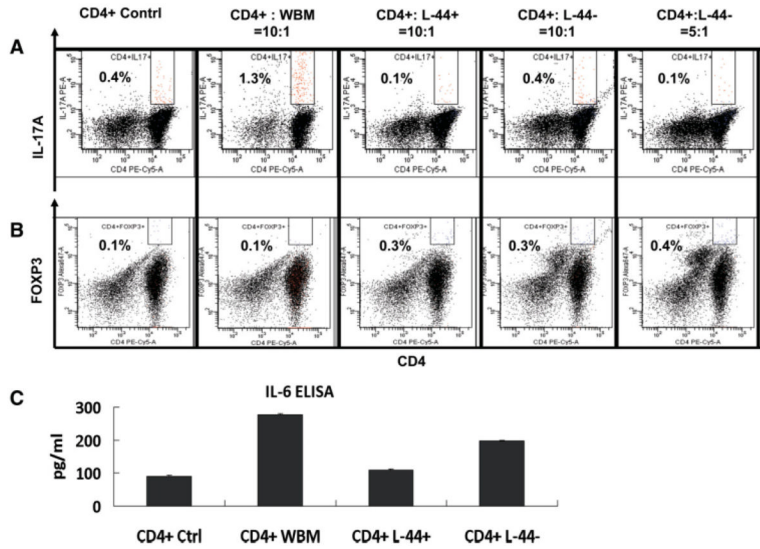


**Figure 3.** Bone marrow-derived  $Lin^{-}CD44^{hi}Sca1^{-}cKit^{+}CD34^{-}$  cells reduce Th17 cells differentiation in activated CD4+ T cells. **(A):** The percentage of CD4+IL-17A+ cells as determined by fluorescence-activated cell sorting (FACS) analysis when CD4+ T cells were cocultured with whole bone marrow (WBM) cells, bone marrow-derived  $Lin^{-}CD44^{hi}Sca1^{-}cKit^{+}CD34^{-}$  (L-44+) cells (ratio of CD4+ to L-44+, 10:1;  $p < .05$ ) or L-44- cells at two different concentrations (ratio of CD4+ to L-44+, 10:1 and 5:1) are shown. **(B):** Percentage of CD4+FOXP3+ cells as determined by FACS when cocultured in similar groups as described above ( $p < .05$ ). **(C):** IL-6 levels from supernatants of CD4+ T cells cocultured in the experiments described above in **(A)**. Groups shown are: CD4+ Ctrl (activated CD4+ T cells alone); CD4+:WBM (CD4+ T cells co cultured with whole bone marrow cells at a ratio of 10:1); CD4+:L-44+ (CD4+ T cells cocultured with L-44+ cells at a ratio of 10:1; CD4+:L-44- (CD4+ T cells cocultured with L-44- cells at a ratio of either 10:1 or 5:1).

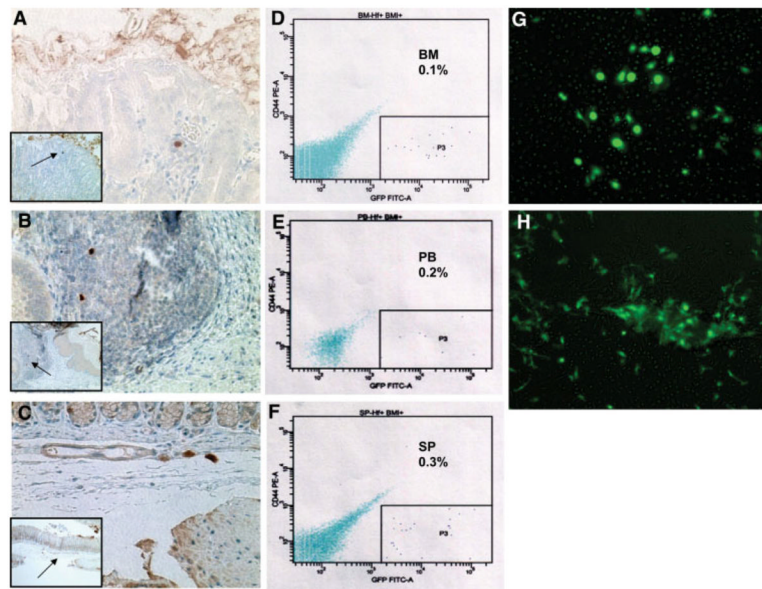


**Figure 4.**

Green fluorescent protein (GFP)-labeled bone marrow-derived Lin<sup>-</sup>CD44<sup>hi</sup>Sca1<sup>-</sup>cKit<sup>+</sup>CD34<sup>-</sup> cells traffic to the bone marrow, peripheral circulation, and the spleen 3 days after infusion into nonirradiated mice. Very few GFP<sup>+</sup> labeled bone marrow derived Lin<sup>-</sup>CD44<sup>hi</sup>Sca1<sup>-</sup>cKit<sup>+</sup>CD34<sup>-</sup> cells trafficked to gastric mucosa (A), lymphoid aggregate (B), and submucosa (C) (400×). (A–C): Anti-GFP staining of 5 μm of formalin-fixed paraffin-embedded gastric sections are shown (low-power field photos are inserted within high-power pictures). (D–F): The majority of the infused cells tracked to the bone marrow (D, 0.1% of 100,000 whole bone marrow cells), blood (E, 0.2% of 10,000 blood mononuclear cells) and spleen (F, 0.3% of 50,000 splenocytes). (G): Infused GFP<sup>+</sup> Lin<sup>-</sup>CD44<sup>hi</sup>Sca1<sup>-</sup>cKit<sup>+</sup>CD34<sup>-</sup> cells were found in the bone marrow 14 days after infusion (3 mice per experiment, 2 experiments, 200×). (H): Mesenchymal stem cells (P3) from the infused GFP<sup>+</sup> cells in bone marrow of recipient mice (200×).

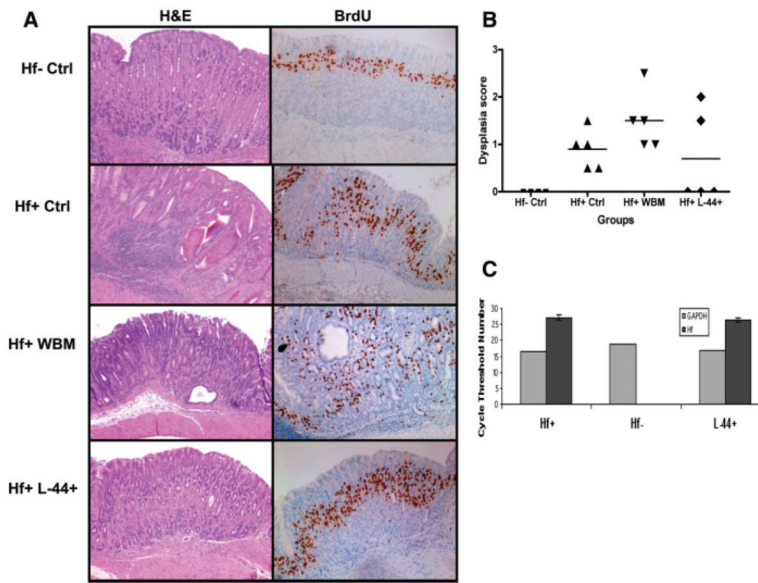


**Figure 5.**

Repeated infusions of bone marrow derived  $\text{Lin}^- \text{CD44}^{\text{hi}} \text{Sca1}^- \text{cKit}^+ \text{CD34}^-$  cells reduce progression to low-grade gastric dysplasia in *Helicobacter felis* infected mice. **(A):** Representative sections of H&E histology and anti-BrdU staining are shown ( $n = 5$  mice per group). Formalin-fixed paraffin-embedded gastric sections, 5  $\mu\text{m}$ , anti-BrdU staining. **(B):** Corresponding distribution of dysplasia scores from each study group are shown (Hf+ Ctrl vs. Hf+ L-44+, chi-square test,  $p = .038$ ). **(C):** Average cycle threshold number of *H. felis* bacterial load as determined by quantitative polymerase chain reaction in Hf+ and Hf+ L-44+ groups is shown ( $n = 5$  mice per group). Abbreviations: Hf-Ctrl, *H. felis* uninfected control; Hf+ Ctrl, *H. felis* infected control; Hf+ WBM, *H. felis*-infected mice with 5,000,000 whole bone marrow cells; Hf+ L-44+: *H. felis*-infected mice with 4 $\times$  infusion of bone marrow-derived  $\text{Lin}^- \text{CD44}^{\text{hi}} \text{Sca1}^- \text{cKit}^+ \text{CD34}^-$  cells.



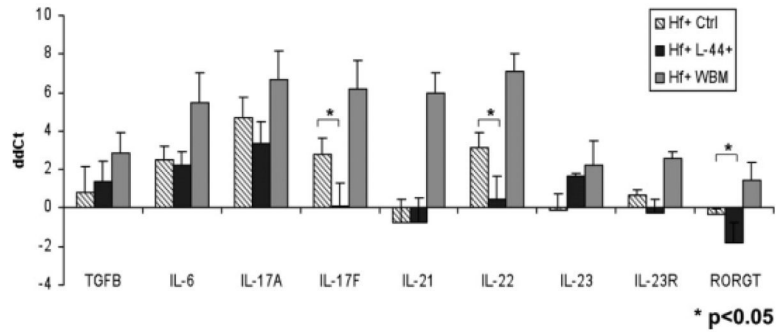


**Figure 6.** Multiple infusions of bone marrow-derived  $\text{Lin}^- \text{CD44}^{\text{hi}} \text{Sca1}^- \text{cKit}^+ \text{CD34}^-$  cells reduces Th17-related proinflammatory gene expression of in the gastric tissue of responding mice. Quantitative polymerase chain reaction analysis showed that gene expression levels of IL-17F, IL-22, and ROR- $\gamma$ t were reduced in the gastric tissue of three responding study mice, which were treated with  $\text{Lin}^- \text{CD44}^{\text{hi}} \text{Sca1}^- \text{cKit}^+ \text{CD34}^-$  cells and did not progress to gastric dysplasia ( $p < .05$ ). Abbreviations: Hf+ Ctrl, *H. felis*-infected control; Hf+ L-44+, *H. felis*-infected mice with bone marrow  $\text{Lin}^- \text{CD44}^{\text{hi}} \text{Sca1}^- \text{cKit}^+ \text{CD34}^-$  cells infusions; Hf+ WBM, *H. felis* infected mice with whole bone marrow cells infusions; ddCt, gene expression level in each study group relative to the uninfected control group.

Table 1

Murine bone marrow transplantation experiments

	<u>Without radioprotective wild-type whole bone marrow</u>			<u>With radioprotective wild-type whole bone marrow</u>		
	4 weeks	4 weeks	4 weeks	4 weeks	4 weeks	16 weeks
<i>n</i>	10	10	3	3	10	10
Mortality (%)	100	100	100	0	0	0
Lin-CD44++ Scal-cKit+ CD34-cells (per mouse)	50,000	50,000	50,000	50,000	50,000	50,000
Wild-type whole bone marrow cells (per mouse)	—	—	—	500,000	500,000	500,000
Green fluorescent protein-positive mesenchymal stem cells	0	0	0	0	3/10	4/10